Am J Transl Res 2019;11(11):6877-6889
www.ajtr.org /ISSN:1943-8141/AJTR0103679

Original Article

Cisplatin induces calcium ion accumulation and hearing loss by causing functional alterations in calcium channels and exocytosis

Jiawen Lu[1,2,3*], Wenxiao Wang[1,2,3*], Hongchao Liu[1,2,3], Huihui Liu[1,2,3], Hao Wu[1,2,3]

[1]Department of Otolaryngology-Head and Neck Surgery, Shanghai Ninth People's Hospital, School of Medicine, Shanghai Jiao Tong University, Shanghai, China; [2]Ear Institute, School of Medicine, Shanghai Jiao Tong University, Shanghai, China; [3]Shanghai Key Laboratory of Translational Medicine on Ear and Nose Diseases, Shanghai, China. [*]Equal contributors.

Received October 18, 2019; Accepted October 29, 2019; Epub November 15, 2019; Published November 30, 2019

Abstract: In recent years, molecular biology and biochemistry have been a focus of studies on the ototoxic side effects of cisplatin. In this paper, the application of cisplatin for 4 h and 72 h was studied from the perspective of electrophysiological function. Patch clamp experiments and immunofluorescence staining were performed on inner hair cells of the cochlea. The patch-clamp results showed that the calcium current amplitude decreased significantly at 4 h and 72 h after cisplatin treatment, the reversal potential was negatively polarized, and the activation time decreased. We suspected that intracellular calcium accumulation was responsible for this result and confirmed this hypothesis by using calpain to measure intracellular calcium concentrations. We tested membrane capacitive function, whose levels after cisplatin application were significantly lower than those in the control group, thus indicating dysfunctional cytoplasmic effervescent function. CtBP2 staining was used to verify this result and indicated a decrease in ribbon synapses. Simultaneously, we observed dysfunction of vesicle circulation after cisplatin application. We found that cisplatin induces the accumulation of calcium ions in inner hair cells by calpain staining and fluoresce intensity calculation, thus decreasing calcium current and synaptic vesicle release, and impairing vesicles cycling, all of which are important mechanisms of cisplatin-induced hearing loss.

Keywords: Cisplatin, ototoxicity, inner hair cell, calcium ions, ribbon synapse, exocytosis

Introduction

Cisplatin chemotherapy has been the primary treatment for cancer since it was approved by the US Food and Drug Administration (FDA) in 1978. It has been widely used as a first-line anti-cancer and chemotherapy drug for ovarian cancer, prostate cancer, testicular cancer, lung cancer, thyroid cancer, head and neck cancer, and esophageal tumors. However, cisplatin has considerable toxic side effects despite its effectiveness in treating cancer. Among these side effects, the ototoxicity of cisplatin is clear: 93% of treated patients have sensorineural hearing loss [1], which leads to permanent hearing loss in 40-80% of patients [2]. Cisplatin enters the inner ear cochlear organ of Corti through several transporters. Owing to the special structure of the cochlea, the drug is not easily cleared through metabolism. Therefore, cisplatin is retained in the cochlea and causes continuous damage to hearing cells [3, 4]. The loss of outer hair cells and spiral ganglia is a serious condition. Although there no clear loss of inner hair cells (IHCs) has been observed, whether their functions might be altered remains unknown [5].

Inner hair cells play an important physiological role as the first station of acoustic signal transmission. Calcium currents and synaptic vesicle release in inner hair cells provide the basis of signal transduction. However, in research on the functional changes in inner hair cells caused by cisplatin, most researchers have focused on molecular biology, whereas relatively little research has been performed on the electrophysiological alterations of inner hair cells, especial-

ly the fine structures, such as synapses, that are important in signal transmission [6-8]. The reason for the absence of electrophysiological studies may be that the cochlea in mammals is buried deep in the temporal bone and has a hard volute covering, thus making collection of materials difficult. Therefore, studies on the electrophysiological functions of auditory organs have mainly focused on the dorsal root ganglia, hippocampus and other central auditory organs that are easily collected [9, 10]. Notably, the patch-clamp technique has not often been used to study the changes in ion channel characteristics of the hair cells of the cochlea. Therefore, in this study, electrophysiological recording was performed directly on the inner hair cells of mice treated with cisplatin to observe the changes in ion channel characteristics. This study focused on the calcium current amplitude and conductance, the activation time of calcium channels and the changes in synaptic vesicle release after short term and long-term cisplatin treatment.

Currently, there are two main hypotheses regarding apoptosis induced by cisplatin: the death receptor pathway and the mitochondrial pathway [11]. Recently, hair cell apoptosis caused by reactive oxygen species generated in cells after medication is administered has been suggested to be a possible mechanism of cisplatin induced hearing injury [12]. In addition, apoptosis through the mitochondrial pathway is a mechanism of cisplatin in the treatment of tumors and may also lead to the apoptosis of cochlear hair cells, thus resulting in sensorineural deafness [13]. However, as described above, the specific mechanism underlying how cisplatin damages the inner hair cell is not yet known. Therefore, this study aimed to establish a reliable model in mice after cisplatin treatment, both 4 h after the acute phase and 72 h after the chronic phase; observe the fine structures of inner hair cells through immunofluorescence staining; and use patch-clamp experiments to observe the changes in calcium influx and membrane exocytosis. We attempted to reveal the mechanism through which cisplatin, through excessive accumulation of calcium ions, leads to an imbalance in calcium influx, the abnormal release of synaptic vesicles and the apoptosis of inner hair cells. This study may provide a reference for the prevention and treatment of ototoxic side effects caused by cisplatin in clinical practice as well as a theoretical basis for relevant pharmacological studies.

Materials and methods

All animal experiments were approved and followed the guidelines of the Animal Care and Use Committee of the Shanghai Jiaotong University School of Medicine (Shanghai, China). In total, 80 C57BL/6 mice, bred in the animal facility at the Shanghai ninth people's hospital, were used in this study.

Establishment of a cisplatin-induced hearing loss mouse model

C57/BL6 mice were treated with a single dose of cisplatin (12 mg/kg, intraperitoneal injection, IP) to induce hearing loss [14]. The optimal ototoxic dose of cisplatin exhibited the desired ototoxicity with an acceptable mortality rate. Specifically, 15 C57/BL6 mice were randomly assigned to the control (pre injection), 4 h after injection and 72 h after injection groups (n = 5 per group). Auditory brainstem response (ABR) thresholds, body weight, MyosinVIIa staining was performed on day 0 and day 3 after cisplatin treatment to verify the effectiveness of the model, as described below.

ABR test

ABRs are auditory evoked potentials derived from the activity of the auditory nerve and the central auditory pathways (brainstem/midbrain regions) in response to transient sound. ABRs were recorded from mice anesthetized with an intra-peritoneal (IP) injection of 480 mg/kg chloral hydrate (Sigma Aldrich-Fluka, St. Louis, MO, USA). Body temperature was monitored and maintained at 37°C with a Homeothermic Monitoring System (Harvard Apparatus, 55-7020, Massachusetts, USA) throughout the experiment. Three needle electrodes were positioned subdermally at the vertex (record), mastoid region (reference) and opposite shoulder (ground). Stimuli were generated with an RZ6 workstation (Tucker-Davis Technologies, Alachua, FL, USA) ranging from 4 kHz to 22 kHz, and a free-field was presented via an MF1 speaker (TDT) 10 cm from the vertex. Differentially recorded signals were amplified (100,000×), band-pass-filtered (0.03-10 kHz) and digitized at a 20 kHz sampling rate

over a 15 ms epoch. The sound level was decreased from a 90 to 0 dB sound pressure level (decibels SPL) in 5-dB steps. Four hundred responses were averaged at each level. Audiograms were determined according to the disappearance of all peaks at 4000 Hz, 5656 Hz, 8000 Hz, 11314 Hz, 16000 Hz and 22627 Hz.

Latencies (ms) and amplitudes (μV) of peak of wave I at 8000 Hz were measured and analyzed between groups in BioSigRZ software (TDT). Latency referred to the time from the onset of the signal to the peak, and amplitude was determined by averaging the ΔV of both sides of the peak.

Whole-mount cochlear staining

Anesthetized mice were euthanized via cervical dislocation, and the cochleae of both sides were harvested and placed in culture dishes with 4% paraformaldehyde in PBS (pH 7.4). A small opening was made at the apex of the cochlea by gently rotating the tip of a needle. The cochleae were quickly perfused with 4% PFA via application to the oval and round windows and the opening at the apex. After fixation overnight at 4°C, cochleae were decalcified with 10% EDTA in phosphate buffered saline for 20-30 h at 4°C, and then the sensory epithelium was dissected and cut into three turns for further immunofluorescence staining. For calpain staining, cochleae were directly dissected into three turns after fixation without decalcification.

After dissection, each cochlear turn was permeabilized and blocked in 10% goat serum/0.1% Triton X-100/PBS at 4°C overnight on a rotator for 60 minutes at room temperature. After incubation with rabbit anti-MyosinVIIa (1:500, 25-6790, Proteus BioSciences Inc) and mouse (IgG1) anti-CTBP2 (1:400, 612044, BD Biosciences) or rabbit anti-calpain 1 (1:100, ab39170, Abcam) and mouse (IgG1) anti-CTBP2 (1:400, 612044, BD Biosciences) at 4°C overnight, all tissues were rinsed three times for 5 minutes in PBS, then incubated with secondary antibodies Alexa Fluor 633-conjugated goat anti-rabbit IgG (H+L) (1:500, A21-124, Invitrogen) or Alexa Fluor 568 goat anti-mouse (IgG1) (1:500, A21070, Invitrogen) at room temperature for 2 h. Both the primary and secondary antibodies were dissolved in 5% goat serum/0.1% Triton X-100/PBS. After being washed three times in PBS, specimens were mounted in ProLongTM Gold Antifade Mountant with DAPI (P36935, Invitrogen) on a glass slide. Images were acquired with a Zeiss LSM 880 laser confocal microscope (Carl Zeiss Microscopy). CTBP2 puncta loss per IHC were measured in three or four different regions of every turn of the cochlea. Calpain intensity was normalized by the control group and analyzed in Imaris 9.3 (Oxford instruments).

Electrophysiological recording

Dissected basilar membranes were placed in a custom-made recording chamber and viewed under an OLYMPUS LUMPlanFL upright microscope (Olympus, Japan) equipped with a 60× water-immersion lens and differential interface contrast optics and filmed with a U-CMAD3 CCD camera (Olympus, Japan). Standard external solution contained (in mM): 106 NaCl, 35 TEA-Cl, 2.8 KCl, 10 HEPES, 5 $CaCl_2$, 1 $MgCl_2$ and 10 D-glucose (300 mOsm/kg, pH 7.40) (adjusted with NaOH). Recording pipettes were pulled from 1B150F-4 borosilicate glass tubes (World Precision Instruments, Sarasota, CA, USA) with a two-stage vertical pipette puller (PC-100; Narishige, Tokyo, Japan). Recording pipettes were coated with dental wax and filled with standard internal solution that contained (in mM): 118.4 cesium methane sulfonate, 10 CsCl, 10 TEA-Cl, 3 MgATP, 0.5 NaATP, 10 HEPES and 2 EGTA (290 mOsm, pH 7.20). Data from hair cells in the apical turns of basilar membranes were recorded with an EPC10 amplifier (HEKA Elektronik, Lambrecht/Pfalz, Germany) driven by a Patchmaster (HEKA Electronics). Cells were held at -80 mV (unless otherwise indicated), and the signals were low pass filtered at 2 kHz and sampled at 20 kHz or higher. Traces were recorded immediately after the cell membrane was broken through at a giga-ohm (GΩ) seal. All electrophysiological recordings were performed at room temperature (23-25°C). Liquid junction potentials were adjusted offline for all membrane potentials. Offline analysis of electrophysiological data was performed primarily with Igor Pro 6.22 software (Wavemetrics, Lake Oswego, OR, USA) and GraphPad Prism 8.0.2 (GraphPad, La Jolla, CA). Most of the stimulus protocols applied in electrophysiology study are described in the figure legends.

Inner hair cell whole cell patch-clamp

Whole-cell membrane capacitance measurements were performed with the lock-in feature and "Sine + DC" method in Patchmaster (HEKA). Sine waves of 1 kHz and 70 mV (peak-to-peak) were superposed on the holding potential briefly. The net increase in Cm before and after stimulation (Δ_{Cm}) was used to assess exocytosis from IHCs in the offline analysis in Igor Pro 6.22 [18].

Conductance-voltage relationships were calculated point-by-point from calcium current responses to ramp the stimulation from -70 mV to +60 mV and fitted to the Boltzmann equation:

$$f(v) = \frac{G_{max}}{1 + e\frac{V_{half} - V}{k_{slope}}}$$

where V is the command membrane potential, G_{max} is the maximum conductance, V_{half} is the half-activation voltage, and k_{slope} is the slope factor that defines the steepness of voltage dependence in current activation. The activation time constant (τ) was determined by fitting a single exponential function to the step stimulation at -5 mV and fitted to the single exponential equation:

$$y = y0 + A\exp\left\{\frac{-(x - x_0)}{t}\right\}$$

Data analysis

Statistical significance was assessed with unpaired Student's t-test (after the reported values passed Kolmogorov-Smirnov normality and log-normality tests (alpha = 0.05)), Ordinary One-way ANOVA followed by Tukey's multiple comparisons test or two-way ANOVA followed by Tukey's multiple comparisons test, and the level of significance was set to P<0.05. All data are reported as mean ± standard deviation (SD) in the text and mean ± standard error of the mean (SEM) in the figures.

Results

Establishment of CDDP treated mice

ABR tests were performed to assess auditory function in control and cisplatin treated mice. **Figure 1A** shows the raw waveform in control and CDDP treated mice. Threshold comparisons revealed significant changes of thresholds in CDDP and control mice (**Figure 1B**). The average thresholds in control group were 56.43 ± 7.48, 42.86 ± 4.88, 36.43 ± 4.76, 25.00 ± 10.00, 22.86 ± 5.67 and 28.57 ± 3.78 in response to 4.0, 5.6, 8, 11, 16 and 22.6 kHz, respectively. The average thresholds were 72.78 ± 4.41, 58.33 ± 9.68, 45.00 ± 8.66, 39.44 ± 6.35, 35.00 ± 5.00 and 42.78 ± 11.76 for the CDDP 4 h mice and 80.00 ± 9.13, 71.00 ± 15.06, 64.50 ± 15.17, 55.00 ± 19.86, 45.50 ± 15.89 and 53.00 ± 14.76 for the CDDP 72 h mice, respectively. Significant differences were found between control mice and both the CDDP 4 h and CDDP 72 h groups at all frequencies, according to two-way ANOVA (P<0.05).

The amplitude and latency of wave I were analyzed at 8000 Hz by measuring the peaks at different intensities (**Figure 1C** and **1D**). Significant differences were observed between the control group and the CDDP 72 h group for the wave I amplitude and latency (P<0.05, two-way ANOVA).

In addition, the body weight changed significantly 72 h after CDDP was injected (P<0.05, one-way ANOVA) (**Figure 1E**).

Inner hair cells stayed intact while outer hair cells were lost after cisplatin administration

Inner and outer hair cells were stained for MyosinVIIa and counted at 0, 4 and 72 h after cisplatin treatment. No significant hair cell loss was observed at 4 h after cisplatin treatment. However, significant outer hair cell loss was observed at 72 h after cisplatin treatment in the apical, middle and basal turns (P<0.05, two-way ANOVA) (**Figure 2A** and **2B**). The inner hair cells remained intact after cisplatin treatment at 4 h and 72 h in all the regions of the basilar membrane.

Cisplatin altered the properties of calcium channels

A voltage ramp from -70 mV to +60 mV was applied, and the Ca^{2+} current response was recorded to investigate the properties of calcium channel (**Figure 3A**). The Ca^{2+} current (I_{Ca}) amplitude was significantly reduced from -206.61 ± 20.89 pA for the control group (n =

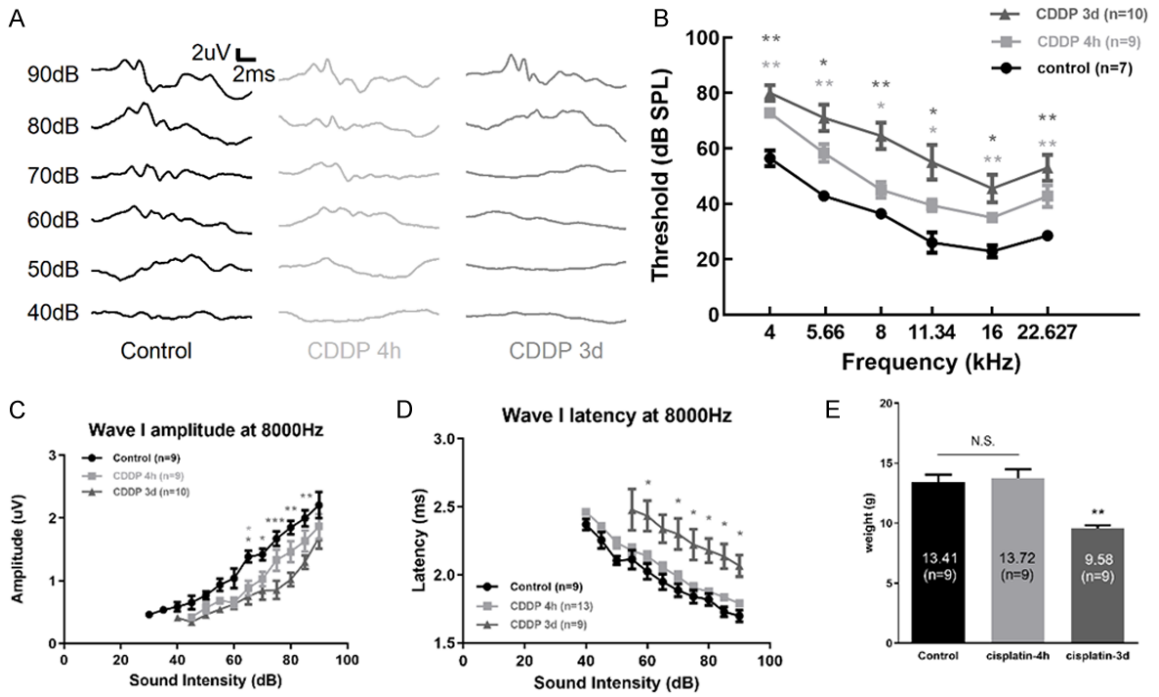

Figure 1. Establishment of a cisplatin-induced hearing loss mouse model. A. Representative auditory brainstem responses (ABRs) recorded from C57/BL6 control and cisplatin intraperitoneally injected mice (single dose (12 mg/kg) after 4 h and 72 h). B. Comparison of ABR threshold shifts after a single dose of intraperitoneal cisplatin. Two-way ANOVA followed by Tukey's multiple comparisons test, *P<0.05, **P<0.01. C and D. Comparison of ABR wave I amplitude and latency at 8 KHz. Two-way ANOVA followed by Tukey's multiple comparisons test, *P<0.05, **P<0.01, ***P<0.001. E. Loss of weight after cisplatin treatment. **P<0.01, one-way ANOVA. For all figures, data are depicted as mean ± SEM, N.S. means P>0.05, *P<0.05, **P<0.01 and ***P<0.001 as compared with the control group. (n, the number of mice used in this experiment).

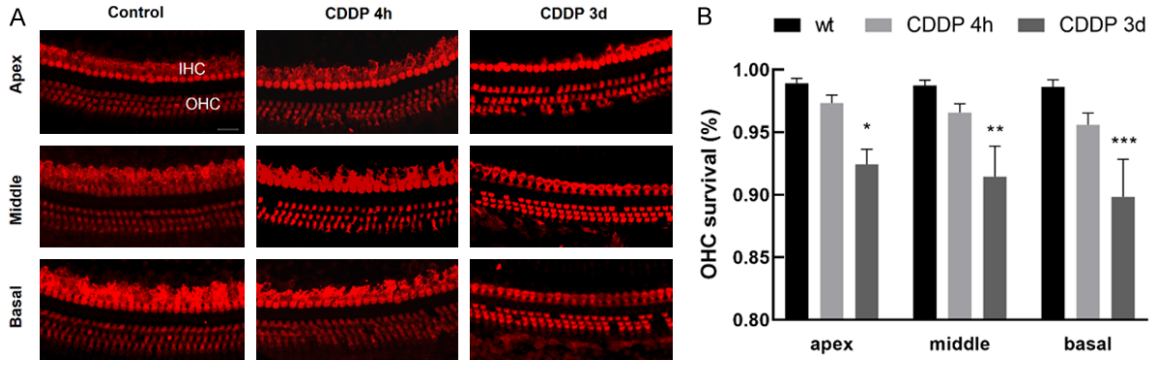

Figure 2. Loss of outer hair cells after cisplatin treatment. A. Representative images show immunolabeling for MyosinVIIa examined 4 h and 72 h after cisplatin injection. Images comprise 40X Z-stack projections taken from the apical, middle and basal turns. Red: MyosinVIIa labeled IHCs; scale bar in bottom-right corner = 20 μm. B. Outer hair cell number changed significantly after 4 h and 72 h of cisplatin treatment. Data are shown as means ± SEM. Two-way ANOVA followed by Tukey's multiple comparisons test, *P<0.05, **P<0.01, ***P<0.001. (Number of mice used in this experiment: 5 for each group).

7) to -145.71 ± 27.69 pA for 4 h (n = 8) and -130.49 ± 27.36 pA for the 72 h group (n = 8) (one-way ANOVA, P<0.001, **Figure 3B**). The reversal potential (Vr) significantly changed from 34.65 ± 4.13 mV in the control group (n = 7) to 29.99 ± 3.85 mV for 4 h (n = 7) and 28.16 ± 4.37 mV in the 72 h group (n = 7) (one-way ANOVA, P<0.05, **Figure 3C**). Normalized

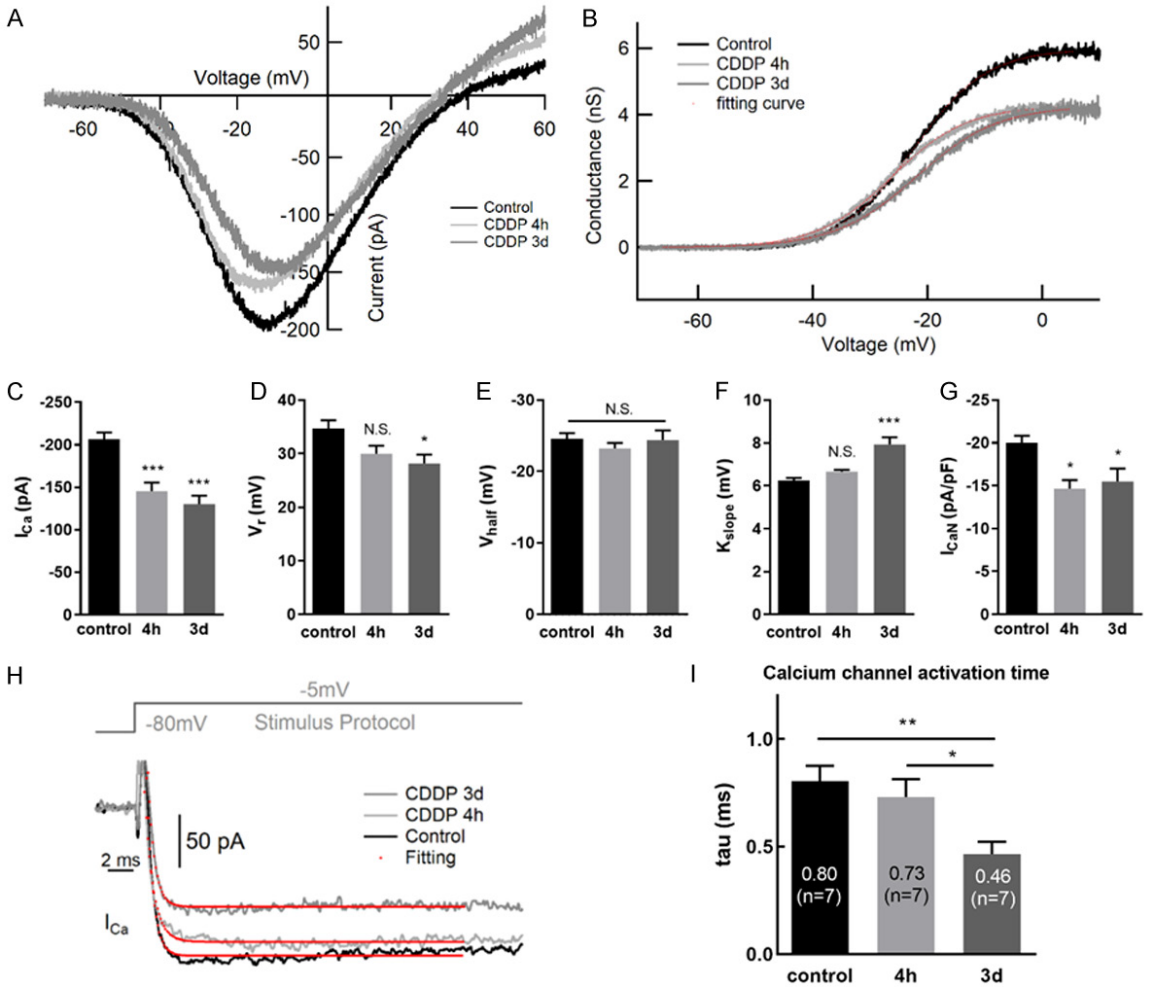

Figure 3. Alterations in calcium currents in inner hair cells of control and CDDP treated mice. (A) Representative calcium currents recorded from three IHCs (control, 4 h and 72 h), induced by a voltage ramp from -70 to +60 mV under a voltage-clamp. (B) According to the Ca^{2+} current shown in (A), the conductance was calculated point by point and plotted against the membrane potential applied. The dashed lines in red depict Boltzmann fitting. (C-G) The Ca^{2+} current in IHCs from cisplatin treated mice has a smaller peak amplitude (C), a more negative reversal potential (D) and a steeper voltage dependency (E). No statistical significance was found in the half-activation voltage of the Ca^{2+} current (V_{half}) among the three groups (F). Normalize calcium currents were shown in (G). (Number of cells used in this experiment: control = 7, CDDP 4 h = 8, CDDP 3 d = 8). (H) Representative calcium currents recorded from three IHCs (control, 4 h and 72 h), induced by a voltage step clamped at -5 mV. The dashed lines in red were fitted with a single exponential equation. (I) A significant difference was found in the activation time constant (τ) of calcium channel from the CDDP 72 h group. *P<0.05, **P<0.01, ***P<0.001, one-way ANOVA.

calcium currents were calculated by dividing the currents to the cell size (I_{CaN} in pA/pF, control: -19.98 ± 2.22; 4 h: -14.68 ± 2.78; 3 d: -15.51 ± 3.19, **Figure 3G**).

We converted I_{Ca} to conductance point by point and fitted the conductance-voltage relationship to the Boltzmann function (**Figure 3B**), thus yielding the half-activation voltage (V_{half}) and the slope of activation (k) for the voltage dependence analysis. We found that I_{Ca} in the 72 h group (7.93 ± 0.95 mV, n = 8) had a steeper activation slope than those of the control (6.25 ± 0.31 mV, n = 7) and 4 h groups (6.66 ± 0.26 mV, n = 8) (P<0.05, one-way ANOVA, **Figure 3E**). Nevertheless, no significant differences were found in the V_{half} among the control, 4 h and 72 h groups (P>0.05, one-way ANOVA, **Figure 3F**).

The activation time (τ) of the calcium channel was calculated by fitting the single calcium current to a single exponential equation (**Figure 3G**) (see methods). Significance was found between the 4 h (0.73 ± 0.22 ms, n = 7) and 72

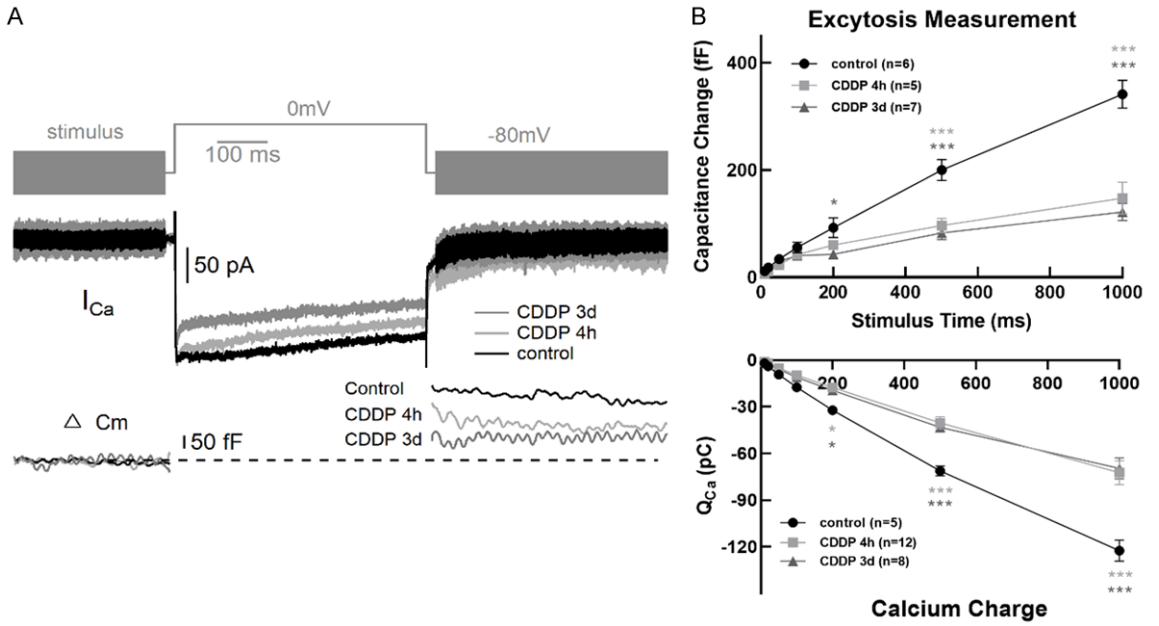

Figure 4. Alterations in exocytosis in inner hair cells of control and CDDP treated mice. A. Representative Ca^{2+} currents and whole-cell capacitance measurements from IHCs (control, 4 h and 72 h). The stimulus protocol is shown on the top panel. Small sine waves were superposed on the holding potential before and after a step depolarization. The step depolarization induced a Ca^{2+} current (I_{Ca}) and triggered exocytosis, which can be quantified with capacitance increase (Δ_{Cm}). B. Both exocytosis (Δ_{Cm}, upper panel) and Ca^{2+} influx (Q_{Ca}, lower panel) are significantly lower in IHCs from cisplatin treated mice. *P<0.05; ***P<0.001. One-way ANOVA followed by Tukey's multiple comparisons test.

h group (0.46 ± 0.15 ms, n = 7) (P<0.05, one-way ANOVA, **Figure 3H**), and the result was more significant between the control (0.80 ± 0.19 ms, n = 7) and 72 h (0.46 ± 0.15 ms, n = 7) groups (P<0.01, one-way ANOVA).

Exocytosis decreased after cisplatin administration

To quantify exocytosis in IHCs before and after CDDP treatment, we applied step stimulation and conducted whole-cell membrane capacitance measurements [15] to determine the membrane area increase (Δ_{Cm}, **Figure 4A**). To examine both the rapid and sustained release of synaptic vesicles, we applied strong depolarizing pulses (i.e., 0 mV, for which the potential resulted in a maximal Ca^{2+} current) and calculated Δ_{Cm} for different stimulation durations from 10 ms to 1000 ms [16, 17]. For rapid and intermediate stimulation of 10, 20, 50 and 100 ms, Δ_{Cm} was similar between the treatment group and the control group (P>0.05, one-way ANOVA, **Figure 4B**; **Table 1**). For longer stimulations, exocytosis was significantly reduced in the 4 h (96.57 ± 32.58 fF vs. control: 200.22 ± 70.55, n = 5, P<0.001 at 500 ms for example, one-way ANOVA) and 72 h (82.56 ± 37.67 fF, n = 5, P<0.05, one-way ANOVA) groups. Moreover, the Ca^{2+} influx, assessed according to the Ca^{2+} charge (Q_{Ca}) was altered in the both 4 h and 72 h group (n = 5, P<0.05 of stimulation from 200 ms to 1000 ms, one-way ANOVA).

To directly examine synaptic vesicle replenishment, we applied double-pulse stimulation (each stimulation depolarized IHCs for 500 ms to maximally deplete synaptic vesicles) with different intervals and built recovery curves of exocytosis for IHCs [18] (**Figure 5**). For an interval of 1000 ms, the Δ_{Cm} in control mice recovered to 0.88 ± 0.12 (n = 7), whereas the Δ_{Cm} in 72 h group mice recovered to 0.58 ± 0.21 (n = 6, P<0.05, one-way ANOVA).

The number of ribbon synapses decreased, and calcium ions accumulated in CDDP treated mice

In this study, we focused on presynaptic ribbons (labeled with CtBP2) [19]. Cisplatin decreased synaptic ribbons at areas correspond-

Table 1. Summary of Δ_{Cm}, Q_{ca}, and Δ_{Cm}/Q_{ca} in IHCs

		10 ms	20 ms	50 ms	100 ms	200 ms	500 ms	1000 ms
Δ_{cm} (fF)	Control	11.43 ± 8.06	18.04 ± 6.96	33.90 ± 13.96	55.57 ± 30.08	92.58 ± 61.17	200.22 ± 70.55	341.40 ± 63.47
	CDDP 4 h	6.34 ± 6.04	11.02 ± 7.81	23.11 ± 7.21	42.18 ± 6.21	60.36 ± 21.01	96.57 ± 32.58	147.73 ± 66.65
	CDDP 3 d	8.42 ± 7.29	13.41 ± 10.61	29.96 ± 5.81	40.32 ± 16.89	43.08 ± 24.82	82.56 ± 37.67	121.76 ± 47.71
P value	control (n = 6) vs. CDDP 4 h (n = 5)	0.9705	0.9390	0.8623	0.7567	0.1545	<0.0001	<0.0001
Tukey's multiple comparisons test	control (n = 6) vs. CDDP 3 d (n = 7)	0.9876	0.9730	0.9743	0.6966	0.0136	<0.0001	<0.0001
	CDDP 4 h (n = 5) vs. CDDP 3 d (n = 7)	0.9950	0.9932	0.9443	0.9952	0.6244	0.7562	0.4270
Q_{ca} (pC)	Control	-1.92 ± 0.22	-3.89 ± 0.54	-9.30 ± 1.20	-17.41 ± 1.02	-32.15 ± 1.60	-71.19 ± 6.86	-122.43 ± 15.09
	CDDP 4 h	-1.03 ± 0.34	-2.02 ± 0.64	-5.11 ± 1.86	-9.72 ± 3.57	-17.51 ± 6.20	-40.27 ± 15.22	-72.36 ± 27.80
	CDDP 3 d	-1.38 ± 0.31	-2.45 ± 0.38	-5.93 ± 0.99	-11.06 ± 1.69	-19.40 ± 3.46	-43.18 ± 9.40	-69.52 ± 21.55
P value	control (n = 5) vs. CDDP 4 h (n = 12)	0.9840	0.9315	0.6954	0.2967	0.0153	<0.0001	<0.0001
Tukey's multiple comparisons test	control (n = 5) vs. CDDP 3 d (n = 8)	0.9945	0.9644	0.8065	0.4677	0.0498	<0.0001	<0.0001
	CDDP 4 h (n = 12) vs. CDDP 3 d (n = 8)	0.9966	0.9956	0.9810	0.9499	0.9053	0.7797	0.7942

Summary of Δ_{cm}, Q_{ca}, and Δ_{cm}/Q_{ca} from patch-clamp recordings in IHCs (**Figure 4**). Data are presented mean ± SD; n = number of IHCs; statistical tests and *p*-values are presented for each dataset.

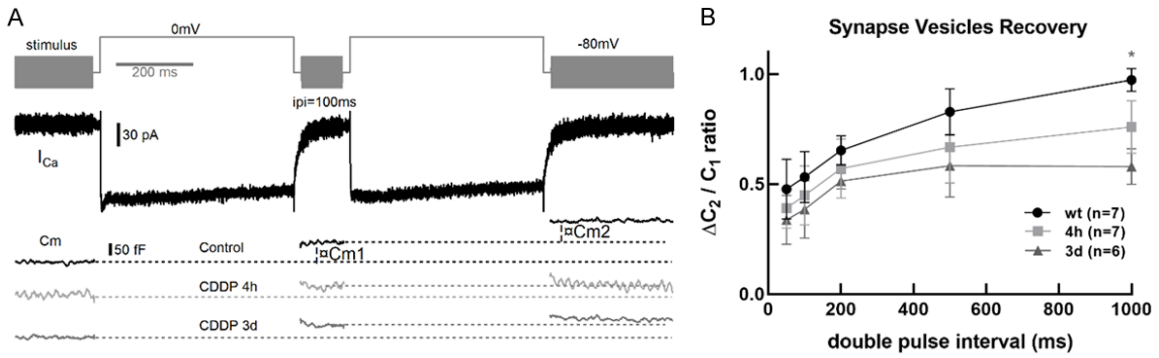

Figure 5. Alterations in synaptic vesicle replenishment in IHCs. A. Representative current responses of three IHCs to double pulse stimulation (control, 4 h and 72 h). Both pulses (500 ms) depleted synaptic vesicles and induced notable I_{Ca} and Δ_{Cm}, and the ratio of $\Delta_{Cm2}/\Delta_{Cm1}$ can be calculated and used to quantify synaptic vesicle replenishment. B. Synaptic vesicle replenishment was significantly slower in IHCs from cisplatin treated 72 h mice. *P<0.05. One-way ANOVA followed by Tukey's multiple comparisons test.

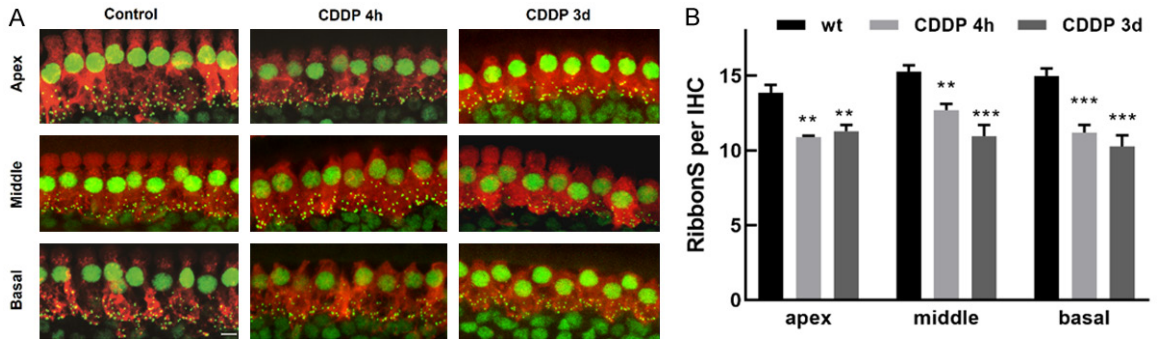

Figure 6. Cisplatin-induced loss of synaptic ribbons after 4 h and 72 h. A. Representative images revealing immunolabeling for CtBP2 examined 4 h and 72 h after cisplatin injection. Images comprise 120X Z-stack projections taken from the apical, middle and basal turn. Red: MyosinVIIa labeled IHCs, green: CtBP2-labeled synaptic ribbons and nuclei of IHCs, blue: DAPI labeled nuclei; scale bar = 5 μm. B. Quantification of CtBP2-immunolabeled ribbon particles in IHCs showed a significant reduction 4 h and 72 h after injection. n = 4 mice per group with one cochlea used per mouse. **P<0.01, ***P<0.001. (Number of mice used in this experiment: 5 for each group).

ing to 4-23 kHz. One-way ANOVA analysis of three groups (control, 4 h and 72 h) showed significant differences at low, middle and high frequency regions (P<0.05) (**Figure 6**).

As shown in **Figure 6**, the number of ribbon synapses per IHC was significantly decreased from 13.86 ± 1.31 (apex, Mean ± SD, N = 6), 15.28 ± 1.04 (middle, N = 6) and 14.98 ± 1.24 (basal, N = 6) for pretreatment to 10.85 ± 0.20 (apex, N = 5), 12.69 ± 1.19 (middle, N = 8) and 11.20 ± 1.16 (basal, N = 5) for 4 h (two-way ANOVA, P<0.01) and to 11.28 ± 0.99 (apex, N = 5), 10.95 ± 1.64 (middle, N = 5) and 10.28 ± 1.79 (basal, N = 6) for 72 h (two-way ANOVA, P<0.01), coinciding with the greatest ABR threshold shift.

We labeled the intracellular calcium ions with calpain I and observed calcium levels (**Figure 7**). In the 4 h and 72 h groups, the calcium ion levels were significantly higher than those in the control group (For basal group after 72 h: 1.47 ± 0.16, N = 4) (P<0.01 compared to control group, P<0.05 for apex and middle group), thus indicating that calcium ions accumulated only in basal turn inside the cochlea after 4 h cisplatin administration and in all turns after 72 h.

Discussion

The exact mechanisms underlying how cisplatin affects the inner hair cells are not fully elucidated [5]. Studies are increasingly focusing on

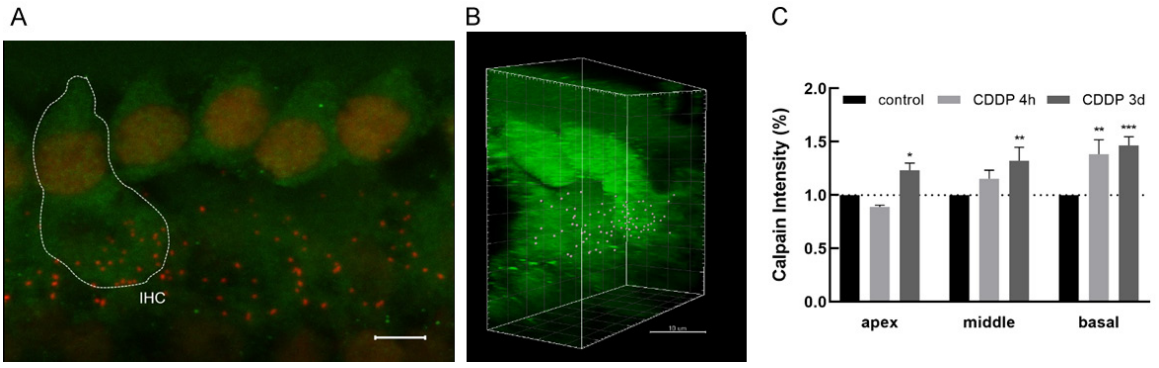

Figure 7. An increase in intracellular calcium concentration in IHCs induced by cisplatin. A. Representative images revealing immunolabeling for Calpain I. Images comprise 189X (63X oil objective and 3X zoom) Z-stack projections. Red: CtBP2-labeled synaptic ribbons and nuclei of IHCs, green: Calpain I labeled calpain proteins; scale bar = 5 μm. B. The CtBP2 region marked by the small white balls was used to calculate the surrounding fluorescence intensity of calpain in Imaris 9.3. C. Calpain I-immunolabeled calcium concentration in IHCs was normalize by the control group and showed a significant increase after 72 h cisplatin injection in all turns inside the cochlea. Significant difference was found only in the basal turn in the 4 h group. n = 4 mice per group with one cochlea used per mouse. *P<0.05, **P<0.01, ***P<0.001. (Number of mice used in this experiment: 5 for each group).

changes regarding molecular biology and biochemistry [6, 20]. In the present study, we studied the plasticity changes in terms of the electrophysiology of inner hair cells in the cochlea.

We choose 12 mg/kg for an optimal dose which exhibited the desired ototoxicity with an acceptable mortality rate [14].

Cisplatin altered the properties of calcium channels in IHCs

Here we generated an ideal cisplatin-induced hearing loss mouse model and investigated the hearing performance and extent of hair cell loss according to cisplatin injection time (after 4 h and 72 h, to determine the short-term and long-term effects). In terms of overall performance, mice injected after 72 h showed a significant loss of appetite, weight and hair, results similar to those from previous studies [21]. In terms of hearing performance, the threshold of the auditory brainstem response shifted approximately 30 dB at all frequencies after cisplatin injection and was accompanied by the loss of outer hair cells (**Figures 1** and **2**). Moreover, the amplitude and latency of ABR wave I decreased while the inner hair cells stayed intact. Given that the sound evoked discharges of all responding afferent fibers were reflected by the amplitude and latency of ABR wave I [22], we wondered whether this decrease might have been due to functional alterations in inner hair cells and a loss of ribbon synapses in IHCs. Ca^{2+} influx through voltage-gated calcium channels triggers precise transmission of auditory signals in IHC ribbon synapses [23], we therefore characterized the biophysical properties of Ca^{2+} channels in IHCs to verify whether function had been altered [24]. We found that the amplitude of I_{Ca} in both the 4 h and 72 h groups was lower than that in the control group. The reversal potential became more negative in the 72 h group (**Figure 3**), thus suggesting that Ca^{2+} channels in 4 h and 72 h IHCs brought less Ca^{2+} into the cell. These results, combined with the finding that I_{Ca} had a steeper slope (k) and shorter activation time constant (τ) in the 72 h group, we hypothesized that calcium ions accumulated in cells under the influence of cisplatin, which affected the equilibrium concentrations of calcium ions inside and outside cells. Therefore, according to the Nernst equation, the inflow of calcium ions outside cells reached equilibrium faster because of the change in concentration gradient. For other changes in calcium channels after cisplatin treatment, although we cannot rule out the possibility of changes in single channel conductance and/or the open probability [25], we favor the interpretation of the reduction of the Ca^{2+} current in IHCs being a result of the loss of ribbon synapses.

Cisplatin perturbed the release and circulation of synaptic vesicles

I_{Ca} has been reported to participate in the regulation of exocytosis of inner hair cells [26]. If cisplatin affects not only the calcium current

but also the exocytosis of inner hair cells, then the results of the hearing loss could be further interpreted. In this study, we varied the stimulation duration from 10 to 1000 ms to study both the rapidly released pool, readily released pool and slowly released pool of ribbon synapses in IHCs after CDDP administration. Cisplatin did not affect the rapid and intermediate exocytosis for stimulation from 10 to 100 ms; however, Δ_{Cm} was significantly lower in both the 4 h and 72 h groups at 200, 500 and 1000 ms than the control group (**Figure 4**), thus indicating that IHCs from the CDDP treated group had fewer synaptic vesicles and a poorer ability to continuously release vesicles. Calcium influx (Q_{Ca}) in IHCs from cisplatin treated mice was diminished (**Table 1** and **Figure 4**), in agreement with the aforementioned finding that I_{Ca} in the treated group had a lower peak amplitude. Hence, we investigated synaptic vesicle replenishment in IHCs by applying a paired pulse protocol for stimulation and used the ratio of the first and second capacitance increase ($\Delta_{Cm2}/\Delta_{Cm1}$) to assess the synaptic vesicle replenishment. As shown in **Figure 5**, the ability of synaptic vesicles to replenishment is weakened and could not recover to 100% after enough rest (with an interval as short as 1000 ms) after 72 h administration of cisplatin. Consequently, cisplatin caused a decrease in the ribbons, thereby leading to a decrease in the number of synaptic vesicles after 72 h administration. However, in contrast, the fast and slow replenishment recovery showed no significant differences between the 4 h group and control group.

Considering that the ABR wave I amplitude represents the sound-evoked discharges of all responding afferent fibers, we wondered whether its reduction might have been due to the loss of ribbon synapses in the inner hair cells. We also estimated the number of ribbon synapses through CtBP2 staining [19] and found that cisplatin led to a decrease in the number of synapses and the number of vesicles released. Moreover, examination of the number of nuclei indicated no apparent loss of IHCs after the cisplatin administration (**Figure 6**).

The accumulation of calcium ions may be the fundamental mechanism through which cisplatin leads to electrophysiological dysfunction in IHCs

Calpain, a calcium-dependent cysteine protease, is activated when intracellular calcium levels increase [27, 28]. In this study we found that the calpain fluorescence intensity increased in the cisplatin treated group. Cisplatin entered in the inner hair cells through stereocilium or cell membrane and caused the increase in intracellular calcium due to the special cochlear structures prevent it from being released, which eventually lead to oxidative stress, inflammation, caspase activation and apoptosis [1]. This suggested that cisplatin treatment might result in accumulation of calcium ions in IHCs and prevent calcium influx according to the Nernst equation. Thus, we propose that the downregulation of calcium currents leads to dysfunction of synaptic release and vesicle replenishment, thereby resulting in hearing loss.

In conclusion, cisplatin appears to inactivate calcium transporters on inner hair cells, thus leading to accumulation of calcium ions, which in turn decrease calcium current amplitude and vesicle release, and consequently result in hearing loss. We will carry out studies on calcium transporters and calcium channel blockers in the future, with the goal of laying a foundation for elucidating pharmacological mechanisms and clinical prevention.

Acknowledgements

This work was supported by two research grants from the National Natural Science Foundation of China to Dr. Hao Wu (81330023 and 81730028) and an institutional research grant from Shanghai Science and Technology Commission to the Shanghai Key Laboratory of Translational Medicine on Ear and Nose Diseases (14DZ2260300). The authors declare no competing financial interests. We thank International Science Editing (http://www.internationalscienceediting.com) for linguistic assistance during the preparation of this manuscript.

Disclosure of conflict of interest

None.

Address correspondence to: Huihui Liu and Hao Wu, Department of Otolaryngology-Head and Neck Surgery, Shanghai Ninth People's Hospital, School of Medicine, Shanghai Jiao Tong University, Shanghai, China. E-mail: liuhent9h@163.com (HHL); haowu@sh-jei.org (HW)

References

[1] Waissbluth S and Daniel SJ. Cisplatin-induced ototoxicity: transporters playing a role in cisplatin toxicity. Hear Res 2013; 299: 37-45.

[2] Breglio AM, Rusheen AE, Shide ED, Fernandez KA, Spielbauer KK, McLachlin KM, Hall MD, Amable L and Cunningham LL. Cisplatin is retained in the cochlea indefinitely following chemotherapy. Nat Commun 2017; 8: 1654.

[3] Rybak LP, Mukherjea D and Ramkumar V. Mechanisms of cisplatin-induced ototoxicity and prevention. Semin Hear 2019; 40: 197-204.

[4] Lu J, Liu H, Lin S, Li C and Wu H. Electrophysiological characterization of acutely isolated spiral ganglion neurons in neonatal and mature sonic hedgehog knock-in mice. Neurosci Lett 2019; 714: 134536.

[5] Wu X, Li X, Song Y, Li H, Bai X, Liu W, Han Y, Xu L, Li J, Zhang D, Wang H and Fan Z. Allicin protects auditory hair cells and spiral ganglion neurons from cisplatin-induced apoptosis. Neuropharmacology 2017; 116: 429-440.

[6] Li Y, Li A, Wu J, He Y, Yu H, Chai R and Li H. MiR-182-5p protects inner ear hair cells from cisplatin-induced apoptosis by inhibiting FOX03a. Cell Death Dis 2016; 7: e2362.

[7] Tani K, Tabuchi K and Hara A. Hair cell loss induced by sphingosine and a sphingosine kinase inhibitor in the rat cochlea. Neurotox Res 2016; 29: 35-46.

[8] Wu X, Li X, Song Y, Li H, Bai X, Liu W, Han Y, Xu L, Li J, Zhang D, Wang H and Fan Z. Allicin protects auditory hair cells and spiral ganglion neurons from cisplatin-induced apoptosis. Neuropharmacology 2017; 116: 429-440.

[9] Kotak VC, Breithaupt AD and Sanes DH. Developmental hearing loss eliminates long-term potentiation in the auditory cortex. Proc Natl Acad Sci U S A 2007; 104: 3550-5.

[10] Lin YW, Min MY, Lin CC, Chen WN, Wu WL, Yu HM and Chen CC. Identification and characterization of a subset of mouse sensory neurons that express acid-sensing ion channel 3. Neuroscience 2008; 151: 544-57.

[11] Manohar S and Leung N. Cisplatin nephrotoxicity: a review of the literature. J Nephrol 2018; 31: 15-25.

[12] Sheth S, Mukherjea D, Rybak LP and Ramkumar V. Mechanisms of cisplatin-induced ototoxicity and otoprotection. Front Cell Neurosci 2017; 11: 338.

[13] Youn CK, Kim J, Park JH, Do NY and Cho SI. Role of autophagy in cisplatin-induced ototoxicity. Int J Pediatr Otorhinolaryngol 2015; 79: 1814-9.

[14] Chen Y, Gu J, Liu J, Tong L, Shi F, Wang X, Wang X, Yu D and Wu H. Dexamethasone-loaded injectable silk-polyethylene glycol hydrogel alleviates cisplatin-induced ototoxicity. Int J Nanomedicine 2019; 14: 4211-4227.

[15] Neher E and Marty A. Discrete changes of cell membrane capacitance observed under conditions of enhanced secretion in bovine adrenal chromaffin cells. Proc Natl Acad Sci U S A 1982; 79: 6712-6.

[16] Hallermann S, Pawlu C, Jonas P and Heckmann M. A large pool of releasable vesicles in a cortical glutamatergic synapse. Proc Natl Acad Sci U S A 2003; 15: 8975-8980.

[17] von Gersdorff H and Matthews G. Dynamics of synaptic vesicle fusion and membrane retrieval in synaptic terminals. Nature 1994; 6465: 735-739.

[18] Liu H, Lu J, Wang Z, Song L, Wang X, Li GL and Wu H. Functional alteration of ribbon synapses in inner hair cells by noise exposure causing hidden hearing loss. Neurosci Lett 2019; 707: 134268.

[19] Schmitz F, Konigstorfer A and Sudhof TC. RIBEYE, a component of synaptic ribbons: a protein's journey through evolution provides insight into synaptic ribbon function. Neuron 2000; 28: 857-872.

[20] Benkafadar N, Menardo J, Bourien J, Nouvian R, Francois F, Decaudin D, Maiorano D, Puel JL and Wang J. Reversible p53 inhibition prevents cisplatin ototoxicity without blocking chemotherapeutic efficacy. EMBO Mol Med 2017; 9: 7-26.

[21] Lin MT, Ko JL, Liu TC, Chao PT and Ou CC. Protective effect of D-methionine on body weight loss, anorexia, and nephrotoxicity in cisplatin-induced chronic toxicity in rats. Integr Cancer Ther 2018; 17: 813-824.

[22] Vlajkovic SM, Ambepitiya K, Barclay M, Boison D, Housley GD and Thorne PR. Adenosine receptors regulate susceptibility to noise-induced neural injury in the mouse cochlea and hearing loss. Hear Res 2017; 345: 43-51.

[23] Zampini V, Johnson SL, Franz C, Knipper M, Holley MC, Magistretti J, Masetto S and Marcotti W. Burst activity and ultrafast activation kinetics of CaV1.3 Ca(2)(+) channels support presynaptic activity in adult gerbil hair cell ribbon synapses. J Physiol 2013; 16: 3811-3820.

[24] Moser T and Beutner D. Kinetics of exocytosis and endocytosis at the cochlear inner hair cell afferent synapse of the mouse. Proc Natl Acad Sci U S A 2000; 2: 883-888.

[25] Alvarez O, Gonzalez C and Latorre R. Counting channels: a tutorial guide on ion channel fluctuation analysis. Adv Physiol Educ 2002; 26: 327-41.

[26] Guillet M, Sendin G, Bourien J, Puel JL and Nouvian R. Actin filaments regulate exocytosis at the hair cell ribbon synapse. J Neurosci 2016; 36: 649-54.
[27] Sorimachi H. Structure and function of calpain and its homologues. Seikagaku 2000; 72: 1297-1315.
[28] Hata S, Sorimachi H and Suzuki K. Structure and function of calpain superfamily. Seikagaku 2001; 73: 1129-1140.